Rab17 Regulates Membrane Trafficking through Apical Recycling Endosomes in Polarized Epithelial Cells

Paola Zacchi,* Harald Stenmark,‡ Robert G. Parton,‖ Donata Orioli,* Filip Lim,§ Angelika Giner,* Ira Mellman,¶ Marino Zerial,* and Carol Murphy*,**

*European Molecular Biology Laboratory, Postfach 10.2209, D-69012 Heidelberg, Germany; ‡Department of Biochemistry, the Norwegian Radium Hospital, Montebello, N-0310 Oslo, Norway; §Centro de Biologia Molecular, Facultad de Ciencias, Universidad Autonoma de Madrid, 28049 Cantoblanco, Spain; ‖Centre for Microscopy and Microanalysis, Department of Physiology and Pharmacology, and Centre for Molecular and Cellular Biology, University of Queensland, 4072 Brisbane, Australia; ¶Department of Cell Biology, Yale University School of Medicine, New Haven, Connecticut 06520; and **Laboratory of Biological Chemistry, Medical School, University of Ioannina, 45110 Ioannina, Greece

Abstract. A key feature of polarized epithelial cells is the ability to maintain the specific biochemical composition of the apical and basolateral plasma membrane domains while selectively allowing transport of proteins and lipids from one pole to the opposite by transcytosis. The small GTPase, rab17, a member of the rab family of regulators of intracellular transport, is specifically induced during cell polarization in the developing kidney. We here examined its intracellular distribution and function in both nonpolarized and polarized cells. By confocal immunofluorescence microscopy, rab17 colocalized with internalized transferrin in the perinuclear recycling endosome of BHK-21 cells. In polarized Eph4 cells, rab17 associated with the apical recycling endosome that has been implicated in recycling and transcytosis. The localization of rab17, therefore, strengthens the proposed homology between this compartment and the recycling endosome of nonpolarized cells. Basolateral to apical transport of two membrane-bound markers, the transferrin receptor and the FcLR 5-27 chimeric receptor, was specifically increased in Eph4 cells expressing rab17 mutants defective in either GTP binding or hydrolysis. Furthermore, the mutant proteins stimulated apical recycling of FcLR 5-27. These results support a role for rab17 in regulating traffic through the apical recycling endosome, suggesting a function in polarized sorting in epithelial cells.

EUKARYOTIC cells continuously endocytose membrane proteins, lipids, and solutes. After internalization, these molecules are selectively recycled back to the cell surface or routed to the degradative pathway. All these sorting events are mediated by a series of heterogeneous and highly dynamic endosomal compartments (for reviews see Watts and Marsh, 1992; Gruenberg and Maxfield, 1995; Mellman, 1996). Separation of recycling receptors from lysosomally directed proteins takes place within the early endosomes, also named sorting endosomes, located in the periphery of the cell (Gruenberg and Maxfield, 1995). From here, recycling molecules can be rapidly transported back to the plasma membrane and, at least in part, transit through a separate network of tubules and vesicles in the pericentriolar region of the cell, whose organization is maintained by microtubules (Hopkins, 1983*a*; Yamashiro et al., 1983; Yamashiro and Maxfield, 1987; Ghosh et al., 1994). These elements represent the so-called recycling endosome (Gruenberg and Maxfield, 1995) or para-Golgi recycling compartment (Yamashiro and Maxfield, 1984). Transit through the recycling endosome proceeds with slower kinetics compared with transport through the early endosome (Yamashiro and Maxfield, 1984; Hopkins et al., 1994). The definition of boundaries between these extremely plastic endocytic structures is controversial, and in some cell types, endosomes appear to form a continuous intricate network spread throughout the cytoplasm (Hopkins et al., 1990). Nevertheless, the association of the small GTPases rab4 (van der Sluijs et al., 1992*a*; Daro et al., 1996) and rab5 (Chavrier et al., 1990; Bucci et al., 1992) with sorting endosomes and rab11 with recycling endosomes (Ullrich et al., 1996), provides support to the existence of functionally and biochemically distinct endosomal compartments.

The organization of the endocytic pathway acquires an

Address all correspondence to Carol Murphy, Laboratory of Biological Chemistry, Medical School, University of Ioannina, 45110 Ioannina, Greece. Tel.: 30 651 97560. Fax: 30 651 67868. E-mail: cmurphy@cc.uoi.gr

Marino Zerial, European Molecular Biology Laboratory, Postfach 10.2209, 69012 Heidelberg, Germany. Tel.: 49 6221 387 232. Fax: 49 6221 387 306. E-mail: zerial@embl-heidelberg.de

additional level of complexity in polarized epithelial cells, which have to maintain a characteristic spatial and functional asymmetry (Simons and Wandinger-Ness, 1990; Nelson, 1992; Rodriguez-Boulan and Powell, 1992; Mostov et al., 1992; Mellman, 1996). The presence of two distinct plasma membrane domains requires separate endocytic and biosynthetic pathways and a communication route that allows transport from one cell surface to the opposite one, i.e., transcytosis (Rodman et al., 1990; Mostov et al., 1992; Mostov, 1994). Studies in polarized MDCK cells have suggested that fluid-phase markers, internalized from the apical or basolateral plasma membrane domain, accumulate in distinct apical and basolateral early endosomes before meeting in late endosomes (Bomsel et al., 1989; Parton et al., 1989; Fujita et al., 1990). However, recent evidence suggested the existence of a single common endosomal compartment that receives markers internalized from both apical and basolateral membranes. Electron microscopy studies in polarized Caco2 cells showed that transferrin (Tf)[1], internalized from the basolateral side, was delivered to an apically located endocytic compartment accessible to apical membrane markers (Hughson and Hopkins, 1990; Knight et al., 1995). In MDCK cells, basolaterally internalized polymeric IgA receptor (pIgR) is first delivered to basolateral endosomes, and then reaches an apical tubular endosomal compartment before being delivered to the apical plasma membrane (Barroso and Sztul, 1994; Apodaca et al., 1994). Altogether these results suggest that, within this structure named the apical recycling compartment (Barroso and Sztul, 1994; Apodaca et al., 1994), recycling receptors and transcytosing molecules are sorted in a polarized fashion. The extent to which apical and basolateral endosomes contribute to polarized sorting, and the exact nature of the apical recycling compartment and its relationship with other portions of the endocytic pathway still remain to be elucidated. Interestingly, however, the apical recycling endosome shares striking similarities with the recycling endosome described in nonpolarized cells: it exhibits a tubular morphology, it is clustered around the microtubule organizing center, and it is reached by membrane markers, such as transferrin receptor (TR; Apodaca et al., 1994), although Barroso and Sztul (1994) failed to detect Tf in this compartment. It is also poorly labeled by fluid phase markers, presumably due to sorting in the early endosomes. These similarities therefore suggest that the apical recycling endosome may be equivalent to the recycling endosome of nonpolarized cells.

How would this compartment function in polarized sorting in epithelial cells? One possibility is that epithelial cells would not require any additional components of the trafficking machinery compared with nonpolarized cells. Fibroblasts already possess elements of the apical and basolateral biosynthetic routes (Musch et al., 1996; Yoshimori et al., 1996), supporting the notion that at least some components involved in cell polarization may exist in nonpolarized cells. Alternatively, the recycling endosome could be modified to function in polarized sorting through the expression of new regulatory molecules.

A small GTPase of the rab family, rab17, has been previously identified to be induced during cell polarization (Lütcke et al., 1993). In developing kidney, rab17 is absent from the mesenchymal precursors, but is expressed upon their differentiation into polarized epithelial cells. Rab17 was localized to the so-called apical dense tubules, vesicular and tubular structures underlying the apical plasma membrane which, based on studies of kidney proximal tubule cells, have been implicated in transcytosis and membrane recycling to the apical surface (Christensen, 1982; Nielsen et al., 1985). Given the important role played by rab proteins in the regulation of membrane traffic (for reviews see Pfeffer, 1994; Nuoffer and Balch, 1994; Novick and Zerial, 1997), the induction of rab17 at the onset of cell polarization may reflect a function in polarized membrane transport.

In the present study we have analyzed the intracellular distribution of rab17 both in nonpolarized BHK-21 cells and in polarized epithelial Eph4 cells (Reichmann et al., 1989; Reichmann et al., 1992). We have found that rab17 associates with the perinuclear recycling endosome when ectopically expressed in nonpolarized cells and with the apical recycling compartment in fully polarized epithelial cells. We have investigated the role of rab17 in receptor trafficking in polarized Eph4 cells expressing wild type rab17 or dominant interfering mutants in an inducible manner. Our results implicate rab17 in the control of transport through the apical recycling endosome and suggest that this GTPase is induced during the generation of cell polarity to link the basolateral and apical endocytic pathways, and to regulate polarized membrane sorting.

Materials and Methods

Cell Culture and Antibodies

Eph4 cells were obtained from H. Beug (Research Institute of Molecular Pathology, Vienna, Austria) and were grown in DME supplemented with 2 mM glutamine, 10% heat-inactivated FCS, 100 U/ml penicillin, and 10 μg/ml streptomycin. For growth on polycarbonate filters, 0.4 μm pore diameter, 12 mm filter diameter (Transwell; Costar Corp., Cambridge, MA), cells were trypsinized, a single cell suspension was made, and seeded at a density of 2.5×10^5 per filter. Medium was placed on both surfaces, 0.5 ml apically and 1.5 ml basolaterally, and was changed daily.

BHK-21 cells were cultured in Glasgow MEM supplemented with 5% heat-inactivated FCS, 10% tryptose phosphate, 2 mM glutamine, 100 U/ml penicillin, and 10 μg/ml streptomycin. All media and reagents for cell culture were purchased from GIBCO BRL (Eggenheim, Germany).

Zo-1 antibody R26.4C was obtained from Developmental Studies Hybridoma Bank (University of Iowa, Iowa City, IA). The antibody for the FcLR 5-27 chimeric receptor was purified from 2.4G2 hybridoma supernatant (Unkeless, 1979) by ammonium sulfate precipitation. Briefly, the 2.4G2 hybridoma supernatant was adjusted to 55% saturation with $(NH_4)_2SO_4$ (Sigma Chemical Co., St. Louis, MO). The precipitate collected by centrifugation was dissolved in H_2O (20 ml of H_2O per liter of supernatant) and dialyzed against protein G binding buffer (10 mM $Na2HPO_4/NaH_2PO_4$ buffer, pH 7.0, 10 mM EDTA, 150 mM NaCl). A preswollen gamma bind plus sepharose column (Pharmacia Diagnostics AB, Uppsala, Sweden) was equilibrated with binding buffer, the sample was applied and bound antibodies were eluted with 0.5 M acetic acid/NH_3, pH 2.5. 1 ml fractions were collected into tubes containing the appropriate volume of 2 M Tris base.

An antibody was raised against a synthetic peptide corresponding to rab17 NH_2-terminal amino acids NH_2-MAQAAGLPQASTASQPK-COOH. The 49-1 antibody was raised against the entire rab17 protein. Rab17 wild

1. *Abbreviations used in this paper*: ECL, electrochemiluminescence; hTR, human transferrin receptor; IFN, interferon; RT, room temperature; Tf, transferrin; TR, transferrin receptor; WT, wild type.

type (WT) was cloned into pRsetA vector (Invitrogen, Carlsbad, CA), transformed into Bl21 DE3 cells, and the expressed protein was purified by nickel agarose affinity chromatography and used to immunize rabbits. For immunofluorescence, the serum was affinity purified using nitrocellulose strips of the recombinant protein. For Western blot analysis the crude serum was used. The antibody against cellubrevin was kindly provided by P. De Camilli (Yale University, New Haven, CT; Galli et al., 1994). All secondary antibodies were obtained from Dianova (Hamburg, Germany).

Preparation and Biotinylation of the Fab Fragment

The purified 2.4G2 IgG was dialyzed against papain buffer (0.1 M NaAcetate, pH 5.5). 6 mg of 2.4G2 IgG were digested with insoluble enzyme as described by the manufacturer (Sigma Chemical Co). Fab fragments were biotinylated with NHS-LC-biotin or NHS-SS-biotin (Pierce, Rockford, IL) after the protocol described by the manufacturer (ImmunoPure NHS-LC-biotinylation Kit; Pierce).

Colocalization of Rab17 and Internalized FITC-Labeled Transferrin in Nonpolarized Cells

DNAs encoding rab17 WT and the human transferrin receptor (Zerial et al., 1986) were cloned into pGEM-1 vector (Promega Corp., Madison, WI) under the T7 promoter. BHK cells were trypsinized 24 h before transfection and seeded onto 11 mm coverslips. Cell were infected with T7 RNA polymerase recombinant vaccinia virus (Stenmark et al., 1995) and cotransfected with both plasmids using DOTAP (Boehringer Mannheim, Mannheim, Germany). 4 h after transfection of the cells in medium devoid of serum the coverslips were incubated in a humidified chamber with 50 μg/ml FITC-labeled transferrin (Ullrich et al., 1993) for 15, 30, or 60 min at 37°C. Coverslips were then rinsed in PBS and fixed in 3% paraformaldehyde, permeabilized with 0.1% Triton X-100, and indirect immunofluorescence was performed to detect rab17. Samples were visualized by confocal microscopy.

Generation of MX-Rab 17 and MX-FcLDL5-27 Expression Constructs

The Mx promoter was excised as a 1.7-kb fragment EcoRI-BamHI from pMXhGH (Hug et al., 1988) and inserted into p163/7 (Woodroofe et al., 1992), from which the H2 promoter had been excised. Mx-rab17 constructs were generated by PCR. A consensus Kozak site (Kozak, 1987) was introduced 5′ to the ATG, and NheI sites were introduced to clone the open reading frame into the Mx expression cassette. The mutations in the coding region of rab17 to generate rab17Q77L and rab17N132I were carried out by PCR-based mutagenesis according to the method of Landt et al. (1990) using oligos 5′-GGGACACAGCCTTCC**T**GGAGAA-GTAC-3′ (rab17Q77L) and 5′-GCTGGTCGGCA**T**CAAAACGG-3′ (rab17N132I).

The FcLR 5-27 chimeric receptor (Matter et al., 1993)–coding region fragment EcoRI-XbaI was excised after changing by PCR the consensus Kozak site 5′ to the upstream methionine, using oligos Fc-KOZ (5′-GAT CGAATTCGCCGCCGCCATGGGAATCCTGCCGTTC-3′) and Fc-Xho primer (5′-CGGGGGCTCGAGTTTGACCACA-3′), and inserted in EcoRI-XbaI sites of pGEM-1 vector (Promega Corp., Madison, WI). Subsequently, the pGEM1 construct was digested with EcoRI-HincII and ligated into the Mx expression cassette EcoRI-SnaBI.

Generation and Characterization of Stable Inducible Eph4 Cell Lines

Eph4 cells were cotransfected in suspension with constructs Mx-rab17 WT, Mx-rab17N132I, or Mx-rab17Q77L and SV40neo for selection using DOTAP (Boehringer Mannheim). Colonies were selected and maintained in 800 μg/ml G418 (geneticin; GIBCO BRL). Expressing colonies were screened by indirect immunofluorescence after induction with interferon (Sigma Chemical Co.). Positive clones were expanded, plated on filter supports (Costar Corp.), and transepithelial resistance was measured. Only those lines with a transepithelial resistance above 2,000 ohm/cm^2 were used for subsequent studies. Zo-1 was also visualized to ensure that the lines were polarized. The lines were subcloned to obtain a high number of expressing cells.

A second round of transfection was carried out to introduce Mx-FcLR 5-27 into the above cell lines. Cotransfection was carried out as above using cells in suspension and SV40-puro (Clontech Laboratories Inc., Palo Alto, CA) as a selectable marker. The colonies were selected in 800 μg/ml G418 and 1 μg/ml puromycin (Sigma Chemical Co.). Clones were screened by indirect immunofluorescence for both rab17 (antibody 49-1) and FcLR 5-27 (monoclonal 2.4G2 antibody). The above polarity checks were then carried out. Clones were expanded and frozen; all assays were performed on early passage cells. Levels of rab17 before and after induction with interferon were also analyzed by Western blot analysis.

Eph4 cells were seeded onto six-well plastic dishes and grown to 80% confluence. One well was induced with interferon and the other left uninduced as a control. After the induction period, the cells were washed in PBS and lysed in 200 μl PBS, 1% SDS, 0.3 mM PMSF (Sigma Chemical Co.), sonicated, boiled for 10 min, and resuspended in loading buffer. Protein content was assayed using the BCA protein assay reagents (Pierce) and BSA as a standard. 20 μg total protein was loaded onto a 12% SDS-PAGE, blotted, and hybridized with a rabbit polyclonal antibody (49-1).

Localization of Rab17 WT Protein in Polarized Eph4 Cells

Eph4 cells, harboring Mx-rab17 WT construct, were grown on filter supports; rab17 was induced with interferon and filters were rinsed in PBS$^+$ (PBS with 1 mM $CaCl_2$ and 1 mM Mg Cl_2) at 37°C, fixed in 3% paraformaldehyde for 15 min at room temperature (RT), permeabilized in 0.1% Triton X-100 for 4 min, and quenched in 50 mM ammonium chloride for 15 min. Filters were then cut from the supports, blocked in 10% FCS for 1 h at RT in a humidified chamber, and rab17 was visualized using an affinity-purified polyclonal rabbit antibody (49-1) followed by FITC-labeled donkey anti–rabbit IgG. Nuclei were visualized with propidium iodide at a concentration of 0.1 μg/ml (Sigma Chemical Co.) for 15 min at RT, after 30 min at RT in 1 mg/ml DNase free- RNaseA (Sigma Chemical Co.). Filter pieces were mounted in 50% glycerol, 100 mg/ml DABCO (Sigma Chemical Co.) with spacers, and sealed with nail varnish. Samples were then analyzed by confocal microscopy.

Rab17 localization was also assayed by immunoelectron microscopy on plastic grown Eph4 cell line harboring Mx-rab17 WT as previously described (Chavrier et al., 1990).

Colocalization of Rab17 and Internalized FITC-labeled Transferrin in Filter-grown Eph4 Cells

Eph4 cells harboring Mx-rab17 WT were grown on filter supports, and expression of rab17 was induced by the addition of interferon for 12 h. The coding region of the human transferrin receptor (hTR) was cloned into the amplicon vector pHSV (Geller and Breakefield, 1988). pHSV- hTR was then packaged into HSV particles as previously described (Lim et al., 1996) and used to infect Mx-rab17 WT-transfected Eph4 cells grown on filter supports (Murphy et al., 1997). Cells were infected in serum-free medium (to deplete transferrin) for 4 h, washed briefly at 37°C, and 50 μg/ml FITC-labeled transferrin was added to the basolateral surface for 90 min at 37°C in a humidified chamber. Cells were then washed briefly, fixed in 3% paraformaldehyde, and rab17 was visualized by indirect immunofluorescence as described below. In the case of the experiment shown in Fig. 5, Eph4 cells were grown on plastic, and human holo-Tf (Sigma Chemical Co.) was internalized for the indicated times at 37°C. After fixation, Tf was visualized using a sheep anti–human Tf serum followed by FITC-labeled anti–sheep IgG and Rab17 with a polyclonal rabbit antibody followed by rhodamine-labeled donkey anti–rabbit secondary antibody.

Colocalization of Rab17 and Internalized Fab Fragment in Eph4 Cells

Fab fragment was prepared as outlined above (preparation and biotinylation of the Fab fragment). Eph4 cells harboring Mx-rab17 WT were plated on coverslips and treated with interferon to induce the expression of both rab17 and the FcLR 5-27. Fab fragment was added to the cells in a volume of 200 μl at a concentration of 7 μg/ml for 5, 10, 20, 40, and 60 min at 37°C. Cells were then rinsed in PBS, fixed, and processed for indirect immunofluorescence. The Fab fragment was visualized using an affinity-purified goat anti–rat IgG F(ab′)$_2$ fragment specific antibody followed by rhodamine-labeled donkey anti–goat secondary antibody. Rab17 was visualized using a polyclonal rabbit antibody followed by FITC-labeled donkey anti–rabbit IgG. Samples were analyzed by confocal microscopy.

Confocal Microscopy, Data Acquisition, and Analysis

Samples were visualized using the EMBL confocal scanning laser beam microscope. Confocal series were carried out at either 0.5 or 1 μm steps. The 529 and 476 laser lines of the Argon-ion laser were used for excitation of rhodamine/propidium iodide and fluorescein, respectively. In the case of Fig. 5, the data were collected on a Leica confocal TCS-NT microscope. Images were recorded and imported into either Adobe Photoshop or NIH Image graphic programs for compilation, and printed directly using the Kodak Color Ease printer.

Endocytosis, Transcytosis, and Recycling of the FcLR 5-27 Chimeric Receptor

Endocytosis and transcytosis mediated by chimeric receptors were assayed as previously described (Hunziker and Mellman, 1989). Briefly, Fab fragments derived from monoclonal antibody 2.4G2 (Unkeless, 1979) were biotinylated with NHS-LC-biotin (Pierce, Rockford, IL) as described above (preparation and biotinylation of Fab fragment section).

Saturating concentrations of biotinylated-Fab fragments (0.5–10 μg/ml) were prebound apically or basolaterally to filter grown Eph4 cells for 1 h on ice. Unbound antibody fragments were removed by washing five times with PBS^+/0.5% BSA and twice with PBS^+. To determine the apical–basolateral surface distribution of the FcLR 5-27 chimeric receptor, the cell surface–associated Fab fragments were eluted with medium containing 0.5% BSA, pH 3.4. To measure intracellular transport, after binding, the cells were incubated for different lengths of time in MEM without phenol red (Sigma Chemical Co.) containing 10 mM Hepes, pH 7.4, and subsequently cooled down on ice. Apically and basolaterally bound antibodies were eluted with medium containing 0.5% BSA, pH 3.4. After 10 min, eluates were collected and elution was repeated once. The pH of these eluates was adjusted to 7.0 by adding 40–60 μl of 1 M Hepes, pH 7.6. The intracellular signal associated with the filters was determined by lysing the cells in KOAc Buffer (115 mM KOAc, 25 mM Hepes, pH 7.4, 2.5 mM $MgCl_2$) containing 1% Triton X-100 and 0.5% SDS. Electrochemiluminescence (ECL) counts of the eluates and lysates were determined as described below. Uptake values represent the amount of signal resistant to acid elution from both surfaces. Transcytosis is calculated as the percentage of signal in the corresponding acid eluate relative to the total amount of originally bound Fab fragment.

To measure recycling of the chimeric receptor to the apical plasma membrane, saturating concentration of Fab fragments reversibly derivatized with biotin (see above) were first preinternalized apically for 10 min at 37°C. The medium was then removed and the cells were further incubated for 10 min at 37°C in the presence of 100-fold excess of nonbiotinylated Fab. Cells were then cooled on ice, washed five times with PBS^+/0.5% BSA, and biotin bound to Fab fragments remaining at the cells surface was stripped by reduction with MesNa (three washes in freshly prepared 50 mM MesNa, 100 mM NaCl, 2.5 mM $CaCl_2$, 50 mM Tris-HCl, pH 7.8, for 20 min followed by three washes with PBS^+ containing 20 mM iodoacetamide; Matter et al., 1993). The cells were incubated in complete medium for various times at 37°C. Biotinylated-Fab fragments, recycled to the apical membrane or transcytozed to the basolateral surface, were eluted and the ECL counts of the eluates and of the lysates were determined as described below.

Nocodazole Treatment

Nocodazole (Sigma Chemical Co.) was dissolved in DMSO at 33 mM stock solution in DMSO, stored at −20°C. Polarized Eph4 cells were either pretreated 3 h at 37°C or 60 min at 4°C after allowing the internalization from the basolateral side of biotinylated Fab fragments for 30 min at 37°C in the presence of 33 μm nocodazole. The apical and basolateral antibody fragments were eluted and quantified. In control experiments, Eph4 cells were incubated in the presence of DMSO alone. Nocodazole did not increase the paracellular diffusion of the Fab fragments in either direction, suggesting that the drug did not affect the integrity of the cell monolayer. Immunofluorescence was also performed to visualize the extent of microtubule depolymerization under the experimental conditions used. Samples were fixed with paraformaldehyde using the pH shift protocol (Bomsel et al., 1989).

Analysis of Transferrin Transport

Iron-saturated human transferrin (Sigma Chemical Co.) was biotinylated with NHS-SS-biotin (Pierce) as previously described (Smythe et al., 1992). Eph4 cells grown either on plastic or on filter supports were serum starved 8 h in DME containing 10 mM Hepes and 0.2% BSA in the presence or absence of interferon. For single round of transferrin cycle experiments, cells were first incubated with 125 nM of biotinylated transferrin in internalization medium (DME, 10 mM Hepes, 0.5% BSA) for 1 h on ice (surface binding). The biotinylated transferrin was added to the basolateral side in the case of filter grown Eph4 cells. After washing six times with cold PBS^+/0.5% BSA cells were incubated with internalization medium for various times at 37°C. The medium of plastic-grown Eph4 cells or the apical and basolateral media of filter-grown Eph4 cells was collected and the surface-bound biotinylated transferrin was stripped by reduction with MesNa (Matter et al., 1993). The intracellular signal associated with the filters was determined by lysing the cells as described above. For continuous uptake experiments, biotinylated transferrin was added to the basolateral medium of filter-grown Eph4 cells for 90 min at 37°C. The apical medium was collected, the cells were extensively washed, and then lysed. The ECL counts of the lysates, and collected media were determined as described below.

The leakage of the cells was controlled in each experiment both with the transferrin receptor and the FcLR 5-27 receptor. In experiments where the ligand was prebound on either side of the monolayer on ice, the excess ligand was washed away and the filters incubated at 37°C for various time intervals. We checked the initial leakage after prebinding by stripping the ligand from both cell surfaces at time zero after washing away excess ligand in duplicate filters. After prebinding and washing away excess ligand, the filters were incubated at 37°C for various lengths of time. For each time point at 37°C, duplicate filters were incubated on ice. The leakage was controlled by stripping the ligand from both cell surfaces at the same time as the 37°C samples were processed. In the experiments where the continuous uptake of transferrin for 90 min at 37°C was quantified, duplicate filters were incubated on ice to check leakage of the monolayer.

Electrochemiluminescence Detection System

The ECL-Analyser System was purchased from Igen Inc. (Rockville, MD). Affinity-purified goat anti–rat IgG F(ab′)2 fragment specific antibody and rabbit anti–sheep IgG were labeled with Origen Tag-NHS (*N*-hydroxysuccinimide ester of a ruthenium chelate; Igen, Inc.) following the protocol described by the manufacturer (Igen, Inc.). The ECL counts of the surface-bound (acid-releasable) and intracellular (acid-resistant) biotinylated Fab for the transcytotic assay were determined as follow: 50 μl of the eluates and lysates were incubated with 4 μg/ml ruthenium-labeled affinity-purified goat anti–rat IgG F(ab′)2 fragment specific antibody for 2 h at RT. Thereafter, 1 μl of M-280 Streptavidin Dynabeads (Dynal, Hamburg, Germany) was added for 15 min at RT. The reaction was stopped by adding 200 μl of assay buffer (Igen Inc.) and samples were directly quantified by the ECL analyzer.

With respect to transferrin trafficking, a different protocol was set up. The samples containing biotinylated transferrin were incubated first with 1 μl of M-280 streptavidin Dynabeads, then with 1.25 μl of sheep anti–human transferrin serum (SAPU, Law Hospital Carluke, Scotland) diluted in 400 μl of wash buffer (50 mM Tris-HCl, pH 7.4, 100 mM NaCl, 2% Triton X-100, 0.2% BSA), and then finally with 2 μg/ml ruthenium-labeled rabbit anti–sheep IgG. All the incubation steps were performed at RT for 1 h. Between the different incubation steps, M-280 streptavidin Dynabeads were washed three times with wash buffer using a Dynal MPC-E Magnetic Particle Concentrator (Dynal, Oslo, Norway). After the last washing step the Dynabeads were resuspended in 100 μl of wash buffer and 100 μl of assay buffer and subsequently quantified by the ECL-analyzer. Both assays were validated by comparing the results to those obtained using iodinated Fab fragment and iodinated transferrin.

Results

Targeting of Rab17 in Nonpolarized Cells

In polarized epithelial cells of the mouse kidney tubules, rab17 was found mainly associated with the basolateral plasma membrane and apical dense tubules (Lütcke et al., 1993). To determine whether rab17 localizes to endocytic organelles, we first studied the targeting of the protein ec-

topically expressed in nonpolarized BHK-21 cells using the vaccinia VT7 system (Bucci et al., 1992). By immunofluorescence confocal microscopy, the bulk of the labeling appeared as a strong focus of fluorescence concentrated in the perinuclear area of the cell and in discrete vesicles dispersed throughout the cytoplasm (Fig. 1, *A*, *D*, and *G*). This staining pattern was reminiscent of the pericentriolar recycling compartment in which Tf and TR accumulate at steady state (Ghosh et al., 1994; Hopkins et al., 1994). We, therefore, investigated whether rab17 positive structures were accessible to internalized Tf. WT rab17 and the human transferrin receptor (hTR) were coexpressed in BHK-21 cells and FITC-Tf was internalized for different lengths of time. As shown in Fig. 1 *B*, after 15 min internalization at 37°C, FITC-Tf localized in peripherally distributed punctate structures, consistent with a localization to early endosomes. At this point, some colocalization with rab17 could be detected (Fig. 1, *A–C*). After 30 and 60 min internalization, however, FITC-Tf concentrated in the pericentriolar area of the cell where it now colocalized with the bulk of rab17 (Fig. 1, *D–F* and *G–I*). Thus, when ectopically expressed in nonpolarized cells, rab17 is primarily targeted to the perinuclear recycling endosome.

Inducible Expression of Rab17 in Polarized Eph4 Epithelial Cells

To study the localization and the functional role played by rab17 in polarized epithelial cells, we took advantage of the Eph4 cell line. Eph4 cells originate from the mammary gland epithelium, by sucloning the previously described IM-2 cell line (Reichmann, 1989) and selecting for pure epithelial single cell colonies. The cells resemble mammary gland luminal epithelium, and can be stimulated under certain conditions to produce β-casein (Strange et al., 1991). Although to date there is almost no data regarding their trafficking properties, we used Eph4 cells instead of the most currently used MDCK cell line for several reasons: (*a*) it responds to mouse interferon; (*b*) both rab17 cDNA and the cell line are derived from the same species (Lütcke et al., 1993), thus avoiding potential problems of mistargeting in nonrodent cell lines (Lütcke, A., and M. Zerial, unpublished observations); (*c*) it contains endogenous rab17 (Fig. 2, *B* and *C*); (*d*) the line is nontumorigenic and, based on the expression of epithelial marker proteins and the high transepithelial resistance, it exhibits a polarized phenotype (Reichmann et al., 1989, 1992). We generated stable Eph4 cell lines which overexpress WT rab17 and two mutants defective in either GTP-hydrolysis (rab17Q77L) or nucleotide binding (rab17N132I). An inducible expression system was used because constitutive expression of dominant interfering mutants of other rab proteins (Bucci et al., 1994) has been reported to be toxic to mammalian cells. For this purpose, the well characterized interferon (IFN)- inducible Mx promoter (Hug et al., 1988; Arnheiter et al., 1990) was chosen because of its tight inducibility (Bachiller and Rüther, 1990; Arnheiter et al., 1990). The rab17 open reading frame was cloned under the control of this promoter, as illustrated in Fig. 2 *A*. The β-globin intron was used to maximize transcription (Woodroofe et al., 1992). Furthermore, we engineered a consensus Kozak site in all constructs to enhance translation efficiency

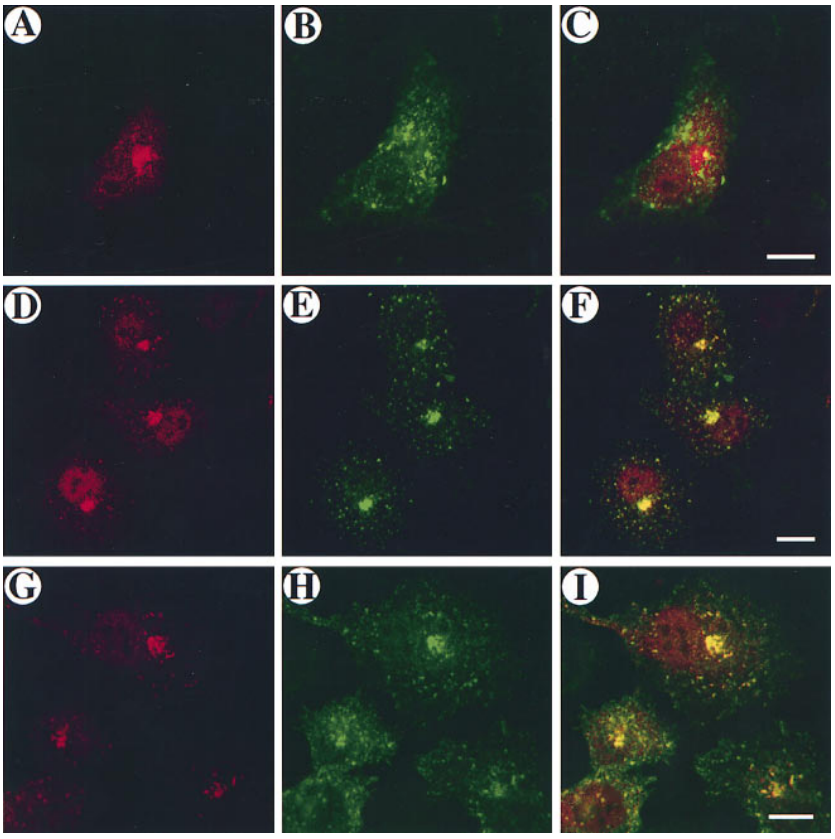

Figure 1. Colocalization of rab17 WT and internalized FITC-labeled transferrin in nonpolarized cells. BHK-21 cells overexpressing rab17 WT and human transferrin receptor by vaccinia infection and transfection (see Materials and Methods) were incubated for 15 (*A–C*), 30 (*D–F*), and 60 min (*G–I*) in the presence of FITC-labeled transferrin. Cells were then fixed, permeabilized, and rab17 was visualized using a polyclonal rabbit antibody followed by rhodamine-labeled donkey anti–rabbit IgG. Samples were analyzed by confocal microscopy. *A*, *D*, and *G* show rab17 staining pattern, *B*, *E*, and *H* show FITC-labeled transferrin distribution, and *C*, *F*, and *I* represent the overlays. Bar, 10 μm.

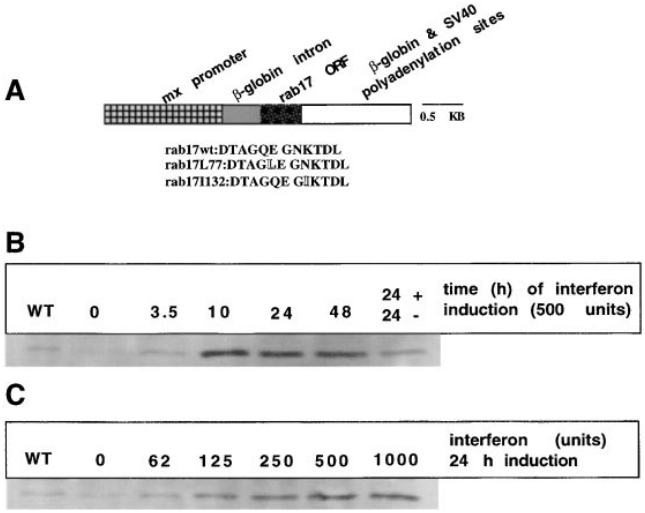

Figure 2. Generation of Eph4 cell lines and characterization of the interferon-inducible system. (*A*) Construct used to generate the Eph4 stable lines overexpressing rab17 WT, rab17Q77L, and rab17N132I. The amino acid changes are indicated in shadow text. (*B*) Time course of protein expression after induction by interferon: protein expression from the Mx promoter was induced with 500 U of interferon. Protein extracts were prepared 0, 3.5, 10, 24, and 48 h after induction, blotted, and probed with a polyclonal antibody recognizing rab17. Finally, after induction for 24 h, interferon was washed out and cells were incubated for a further 24 h in the absence of interferon. (*C*) Concentration of interferon required for maximum protein expression: protein expression was induced with increasing units of interferon from 0 to 1,000 U per ml. Protein extracts were prepared 24 h after induction, blotted, and probed with a polyclonal antibody recognizing rab17.

(Kozak, 1987). Time and dose dependence of expression were assayed by Western blot analysis. Treatment of Eph4 cells grown on plastic support for 24 h with increasing amounts of IFN led to a concentration-dependent expression, reaching a plateau at 500 U (Fig. 2 *C*). To estimate the time course of expression, Eph4 cells were induced with 500 U of IFN for various lengths of time. Protein expression was detected already at the earliest time point investigated (3.5 h) and was maximal after 10 h of induction (Fig. 2 *B*). Moreover, by confocal immunofluorescence microscopy analysis performed on Eph4 cell lines grown on filter support, rab17 was confirmed to be homogeneously expressed in the cells (not shown). For all the experiments reported here, Eph4 cells were incubated for 8 h in the presence of 500 U of IFN.

Intracellular Distribution of Rab17 in Polarized Eph4 Cells

The subcellular localization of rab17 was then examined in filter-grown Eph4 cells harboring Mx-rab17 WT by immunofluorescence confocal microscopy. Serial sections were recorded from the apical region of the cell just below the apical brush border (Fig. 3, *A–C*), above (Fig. 3, *D–F*) and at the level of the nucleus (Fig. 3, *G–I*), from the lateral surface of the cell (Fig. 3 *J–O*) and from the basal portion of the cell (Fig. 3, *P–R*). Rab17 appeared to be concentrated in vesicular and tubular elements at the apical pole

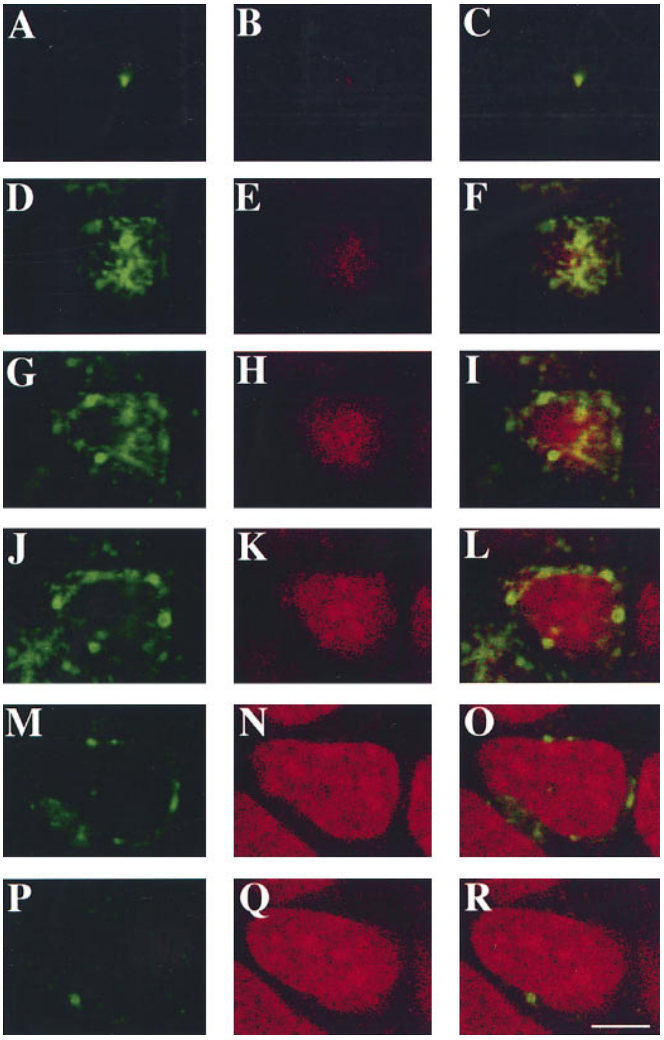

Figure 3. Localization of rab17 WT protein in polarized Eph4 cells. Eph4 cells were grown on filter supports, rab17 WT was induced with interferon, and cells were fixed and processed for confocal analysis. Cells were fixed, permeabilized, and rab17 was visualized using a polyclonal rabbit antibody followed by FITC-labeled donkey anti–rabbit IgG (*A*, *D*, *G*, *J*, *M*, and *P*). Nuclei were visualized with propidium iodide (*B*, *E*, *H*, *K*, *N*, and *Q*). *C*, *F*, *I*, *L*, *O*, and *R* represent the overlays. Samples were analyzed by serial sectioning from the apical cell surface (ACS; *A–C*) and the following sections are shown: 1.6 μm below the ACS (*D–F*), 2.4 μm below the ACS (*G–I*), 3.2 μm below the ACS (*J–L*), 5.6 μm below the ACS (*M–O*), and 8.4 μm below the ACS (*P–R*). Bar, 5 μm.

of the cell above the nucleus and underneath the apical plasma membrane, as previously shown on mouse kidney sections (Lütcke et al., 1993). These structures extended also towards the lateral side, but the signal was undetectable on the basolateral plasma membrane. The lack of labeling on the basolateral plasma membrane is in contrast with what we previously observed in kidney cells (Lütcke et al., 1993). The reasons for this discrepancy are not clear and could be due to antibody reactivity or differences in

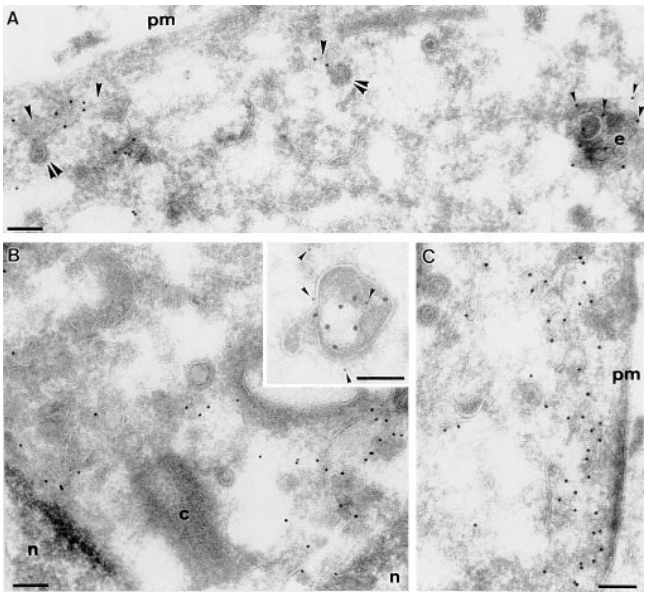

Figure 4. Immunoelectron microscopic localization of rab17 in Eph4 cells. Cryosections of Eph4 cells were labeled with antibodies to rab17 followed by 10 nm protein A-gold. Labeling is associated with tubulovesicular elements (*A–C*), as well as with multivesicular endosomes (*e*, land *A*; also see *inset* in *B*). Labeled tubulovesicular elements were frequently observed underlying the plasma membrane (*pm*) and close to centrioles (*c*, lane *B*). As shown in *A*, the rab17-positive tubulovesicular elements were sometimes seen to be in continuity with putative clathrin–coated buds, although the coated regions were invariably rab17-negative. Double labeling with antibodies to cellubrevin followed by 5 nm protein A–gold (*inset*, *B*) showed some colocalization of cellubrevin (small gold, *arrowheads*) and rab17 (large gold). *n*, nucleus. Bars, 100 nm.

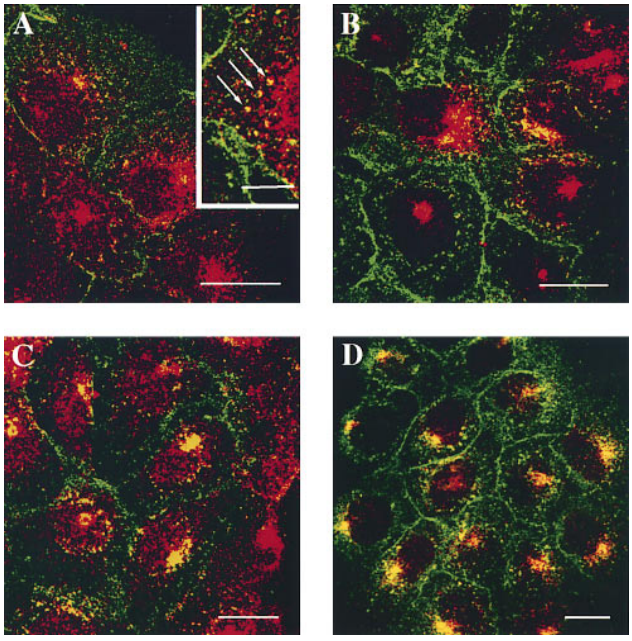

Figure 5. Colocalization of rab17 WT and internalized holotransferrin in Eph4 cells grown on plastic. Holo Tf was internalized for 5 (*A*), 15 (*B*), 30 (*C*), and 60 min (*D*) at 37°C in Eph4 cells harboring Mx-rab17 WT after induction with interferon. Inset in *A* show at high magnification structures where rab17 and transferrin colocalize (*arrows*). Cells were fixed and Tf was visualized using a sheep anti–human Tf serum followed by FITC-labeled anti–sheep IgG. Rab17 was visualized using a polyclonal rabbit antibody followed by rhodamine-labeled donkey anti–rabbit secondary antibody. Bars, 20 μm; *inset*, 10 μm.

steady state distribution in various cell types. Most importantly, the staining pattern in the apical region is strikingly similar to that of the apical recycling endosome, which is normally located around the centrosome (Apodaca et al., 1994; Mostov and Cardone, 1995). Also, in the case of rab17 immunoelectron microscopy analysis on Eph4 cells, harboring Mx-rab17 WT grown on plastic showed the presence of the protein on tubular structures, which surround the centrosome (Fig. 4 *B*), on vesicular elements located close to the plasma membrane (Fig. 4, *A* and *C*), and on multivesicular endosomal structures (Fig. 4, *A* and inset *B*). These latter structures were positive for the synaptobrevin/VAMP–related protein cellubrevin (McMahon et al., 1993; Galli et al., 1994; Daro et al., 1996), a membrane protein ubiquitously distributed along the receptor-mediated endocytic pathway, confirming the endosomal nature of rab17-labeled elements.

Transferrin Internalized from the Basolateral Cell Surface Colocalizes with Rab17 in an Apical Endosomal Compartment

Because it has been reported that at least a fraction of TR, internalized from the basolateral surface into basolateral early endosomes, accesses the apical recycling compartment (Apodaca et al., 1994), we initially assayed whether this molecule would enter the rab17-positive compartment in Eph4 cells. In the first part of our analysis we used semi-polarized cells grown on coverslips to gain maximal sensitivity of detection of the fluorescent markers. The distribution of human holo-Tf internalized in Eph4 cells overexpressing WT rab17 for various times at 37°C was compared with that of rab17 by double-label confocal immunofluorescence microscopy. Afer 5 min uptake, Tf was present in punctate structures dispersed throughout the cell periphery, whereas the bulk of rab17 was concentrated in the perinuclear compartment with some label also in small peripheral vesicles radiating from it. Only few of these structures also contained Tf (Fig. 5 inset *A*), suggesting that rab17 is not enriched in basolateral early endosomes. After 15 min internalization, only a small fraction of Tf reached the rab17 in the pericentriolar recycling endosome. Interestingly, little colocalization at this time point was especially observed in more confluent and polarized cells where the rab17 positive compartment was positioned above the nucleus (Fig. 5 *B*). However, the colocalization increased after 30 and 60 min, when Tf progressively entered the rab17-positive strucures located on the apical pole of the cells (Fig. 5, *C* and *D*).

To examine the accessibility of the rab17 positive compartment to Tf in fully polarized Eph4 cells, the human TR was transiently overexpressed using a recombinant herpes virus (Geller and Breakefield, 1988), as the endogenous labeling was too low to be detected in filter-grown cells

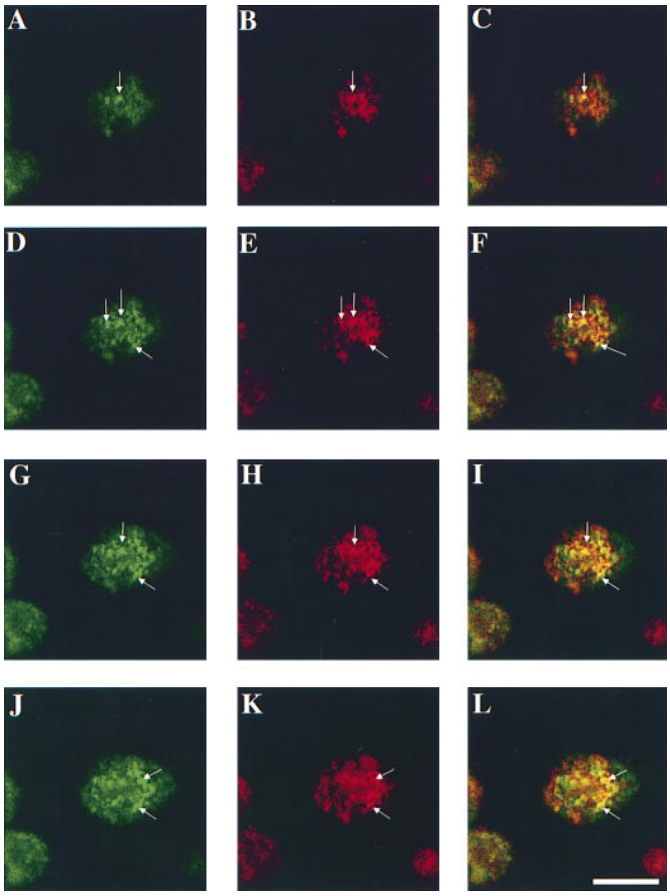

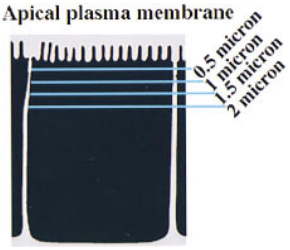

Figure 6. Colocalization of rab17 and internalized FITC-labeled transferrin in polarized epithelial cells. Eph4 cells harboring Mx-rab17 WT were grown on filter supports, induced with interferon to express the rab17 protein and FITC-labeled transferrin was internalized from the basolateral surface for 90 min at 37°C. Cells were washed, fixed, and rab17 was visualized using a polyclonal rabbit antibody followed by rhodamine-labeled donkey anti–rabbit IgG. Samples were analyzed by confocal microscopy. *A*, *D*, *G*, and *J* show FITC transferrin; *B*, *E*, *H*, and *K* show rab17; and *C*, *F*, *I*, and *L* represent the overlays. Samples were serially sectioned from the ACS and as shown in the diagram to the right, *A–C* are 0.5 μm, *D–F* 1 μm, *G–I*, 1.5 μm, and *J–L*, 2 μm below the ACS. Bar, 10 μm.

(data not shown). The coding region of the hTR was cloned into pHSV-1 amplicon vector, and was subsequently packaged using a replication-incompetent HSV-1 helper virus in a permissive cell line (Lim et al., 1996). The virus produced was used to infect Eph4 cells harboring Mx-rab17 WT construct (Murphy et al., 1997). To compare the distribution of rab17 with the intracellular compartments that TR has access to at steady state, FITC-Tf was basolaterally internalized for 90 min at 37°C. Confocal sections scanning specifically the apical region of the cells, each 0.5 μm apart, are shown in Fig. 6. A significant degree of colocalization between rab17 staining and basolaterally internalized Tf was observed throughout the apical most region of the cells (Fig. 6, *C*, *F*, *I*, and *L*, *arrows*). In addition, some structures labeled for rab17 could be observed that were poorly labeled with FITC-Tf, indicating that rab17 resides on apical structures that are not accessible to, or enriched in FITC-Tf endocytosed from the basolateral side. These results indicate that rab17-positive apical structures, at least partially, overlap with the apical endosomal compartment accessible by Tf internalized from the basolateral membrane. It has been speculated that the apical recycling endosome may correspond to the recycling endosome described in nonpolarized cells (Apodaca et al., 1994). Given that rab17, when ectopically expressed in nonpolarized cells, localizes to perinuclear recycling endosomes, these results provide support for the hypothesis that recycling endosome and apical recycling compartment are homologous organelles.

Effect of Rab17 Mutants on Transferrin Recycling

Given that internalized Tf is able to reach rab17-positive endosomal structures both in nonpolarized and polarized cells, we analyzed whether the overexpression of WT and mutant rab17 proteins would affect the Tf cycle. Because Eph4 cells display low levels of TR, we used a highly sensitive nonradioactive detection system based on ECL technology to quantify the kinetics of Tf internalization and recycling without the need to overexpress TR (see Materials and Methods). The Tf cycle was initially studied in plastic-grown Eph4 cells treated with or without IFN to compare the kinetics in the presence or absence of rab17 proteins. Biotinylated Tf was first bound on the surface at 4°C, and then internalized by shifting the cells to 37°C. Fig. 7 shows the kinetics of the Eph4 clone overexpressing the rab17N132I mutant protein (Fig. 7, *A* and *B*). In all cell lines tested, prebound transferrin was rapidly endocytosed and efficiently recycled back to the plasma membrane. The measured rates are similar before and after induction of the rab17 proteins, indicating that the Tf cycle is not affected by the overexpression of WT and mutants rab17 in nonpolarized Eph4 cells.

We then performed similar experiments in polarized rab17N132I Eph4 cell lines grown on filter supports. Tf endocytosis and basolateral recycling were similarly unaffected (Fig. 7, *C* and *D*). In contrast, we observed a small but significant increase of apically released Tf in cells expressing rab17Q77L and rab17N132I mutants (data not shown), which was neither seen in the case of WT rab17

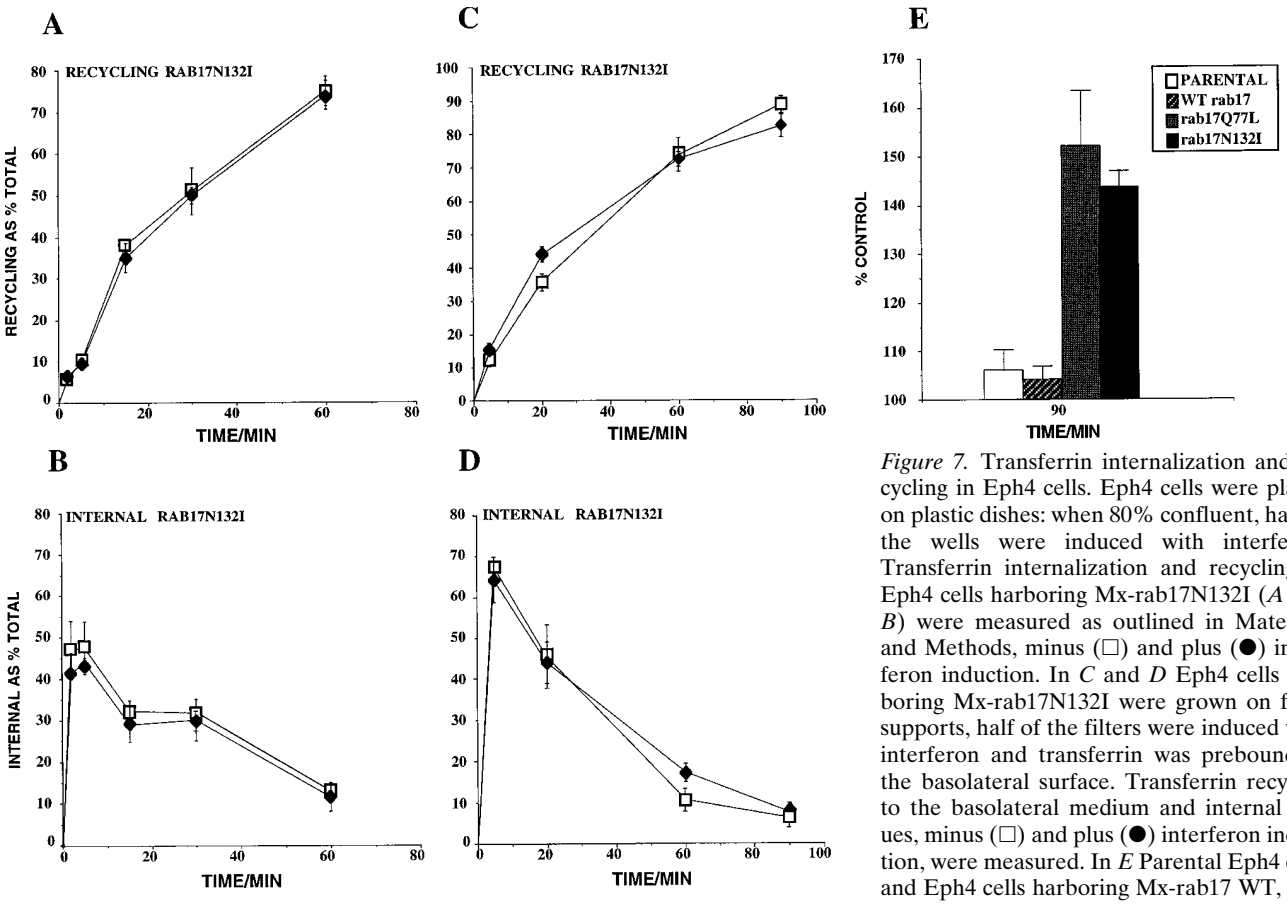

Figure 7. Transferrin internalization and recycling in Eph4 cells. Eph4 cells were plated on plastic dishes: when 80% confluent, half of the wells were induced with interferon. Transferrin internalization and recycling in Eph4 cells harboring Mx-rab17N132I (*A* and *B*) were measured as outlined in Materials and Methods, minus (□) and plus (●) interferon induction. In *C* and *D* Eph4 cells harboring Mx-rab17N132I were grown on filter supports, half of the filters were induced with interferon and transferrin was prebound to the basolateral surface. Transferrin recycled to the basolateral medium and internal values, minus (□) and plus (●) interferon induction, were measured. In *E* Parental Eph4 cells and Eph4 cells harboring Mx-rab17 WT, Mx-rab17Q77L, and Mx-rab17N132I were grown on filter supports and half of the filters were induced with interferon. Transferrin was continuously internalized from the basolateral surface for 90 min at 37°C. Then the cells were rapidly cooled on ice, the apical media collected, and measured as previously described (see Materials and Methods). The given values represent the mean of duplicate samples expressed relative to the same cell line without interferon induction; the experiments were repeated three times with similar results.

protein overexpression, nor was it due to the IFN induction itself (data not shown).

To better follow the trafficking of transferrin to the apical cell surface, we changed the experimental conditions in order to follow multiple transferrin cycles. Tf was continuously internalized from the basolateral surface for 90 min at 37°C. At this time point, the fraction of transferrin released by Eph4 cells into the apical medium in the absence or presence of IFN was ~19% of the total cell associated (surface-bound and internal). The amount recovered in the apical medium of the various Eph4 cell lines was expressed as a percentage of the same cell line before induction with IFN. As shown in Fig. 7 *E*, we detected a 50% increase of apically released Tf in cells overexpressing rab17 mutants compared with uninduced or control cells, indicating that interfering with the function of rab17 causes an increase of Tf release into the apical medium. The effect on Tf transcytosis was observed only after induction of the rab17 mutant proteins. The lines harboring the mutant proteins had a similar receptor number to the Eph4 parental line or the line expressing rab17 WT, ruling out the possibility that the increased apically released Tf may be due to increased receptor number.

FcLDL Receptor Chimera Has Access to Rab17-positive Endosomal Compartment

The observation that a fraction of TR is transcytosed apically in response to the expression of rab17 mutants, prompted us to investigate more closely the transcytotic pathway in these cells. To this end, we took advantage of the FcLR 5-27 (Matter et al., 1993), a chimeric receptor in which the extracellular and the transmembrane domain of the mouse IgG Fc receptor have been fused to the cytoplasmic tail of the LDL receptor deleted of the distal basolateral sorting determinant (Matter et al., 1993). When expressed in MDCK cells, this receptor is targeted to both apical and basolateral plasma membrane domains. In this way it is possible to determine apical and basolateral uptake and transcytosis occurring in both directions (apical to basolateral and basolateral to apical; Matter et al., 1992, 1993). We measured the receptor traffic using a well characterized high affinity Fab fragment of the anti-FcRII monoclonal antibody 2.4G2 as a pseudoligand (Unkeless, 1979; Mellman and Plutner, 1984*a*; Mellman et al., 1984*b*).

We intended to constitutively express the FcLR 5-27 in the above described rab17 Eph4 cell lines. However, all attempts were unsuccessful, and we, therefore, inducibly ex-

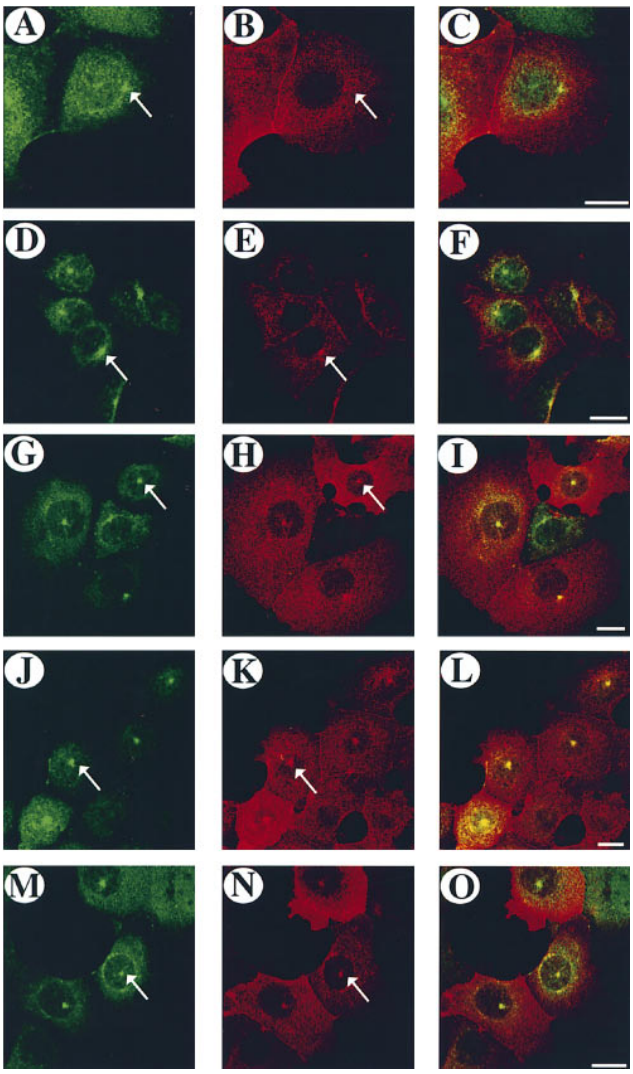

Figure 8. Colocalization of rab17 and internalized Fab fragment. Fab fragment was internalized for 5 (*A–C*), 10 (*D–F*), 20 (*G–I*), 40 (*J–L*), or 60 min (*M–O*) at 37°C in Eph4 cells harboring Mx-rab17 WT and Mx-FcLR 5–27 receptor constructs after induction with interferon. Cells were fixed and the Fab fragment was visualized by indirect immunofluorescence, using a goat anti–rat IgG $F(ab')_2$ fragment specific antibody followed by rhodamine labeled donkey anti–goat secondary antibody. Rab17 was visualized using a polyclonal rabbit antibody followed by FITC-labeled donkey anti–rabbit IgG. Samples were analyzed by confocal microscopy. *A*, *D*, *G*, *J*, and *M* show rab17 staining pattern, *B*, *E*, *H*, *K*, and *N* represent the Fab staining pattern and *C*, *F*, *I*, *L*, and *O* represent the overlays. Bars, 20 μm.

pressed the receptor using the Mx promoter. Eph4 cell lines harboring Mx-rab17 constructs were subsequently stably transfected with the Mx-FcLR 5-27 construct and selected for inducible expression of the protein.

We first verified that, as predicted, the FcLR 5-27 would reach the rab17 positive compartment. The intracellular localization of the FcLR 5-27 was assayed in plastic-grown Eph4 cells overexpressing WT rab17 by continuous uptake of the Fab fragment for different lengths of time. After 5 min of internalization at 37°C the Fab fragment labeling was dispersed throughout the cytoplasm in small discrete vesicles, some colocalizing with rab17 (Fig. 8, *A–C*), but after 10 min a small fraction of the Fab fragment started to enter the rab17-positive compartment in the perinuclear area of the cell (Fig. 8, *D–F*). The colocalization of internalized Fab fragment and rab17 significantly increased after 20 min of internalization (Fig. 8, *G–I*) and was maximal at 40 and 60 min at 37°C (Fig. 8, *J–L* and *M–O*). These results show that FcLR 5–27 does access the rab17-positive compartment, indicating that it is a suitable marker to further investigate the transport steps regulated by rab17.

Rab17 Mutants Affect Transcytosis of the FcLDL 5-27 Receptor

We next analyzed the effect of rab17 mutants on FcLR 5–27 trafficking along both apical and basolateral endocytic pathways. As in the case of transferrin measurements, we made use of a nonradioactive detection system to determine the amount of Fab fragment surface bound, endocytosed and transcytosed by the Eph4 clones. Biotinylated Fab fragments of the anti-FcRII antibody were prebound either at the apical or at the basolateral surface of the Eph4 cells. After extensive washing, cells were incubated for different times at 37°C and surface-bound antibody fragments were eluted from both plasma membrane domains by low pH treatment. The remaining Fab fragment therefore represents the fraction of internalized receptor. In the Eph4 clone control the distribution of the receptor on the surface was 19% apical and 81% basolateral. This was similar to the distribution in Eph4 cells expressing rab17WT (25% apical and 75% basolateral). However, in rab17Q77L and rab17N132I expressing cell lines more receptor was found on the apical surface (32% apical, 68% basolateral and 42% apical, 58% basolateral, respectively). Thus, the mutant proteins altered the apical–basolateral distribution of the FcLR 5-27.

In all Eph4 clones expressing rab17Q77L and rab17N132I examined, the chimeric receptor was efficiently internalized at both apical and basolateral surfaces, as presented in Fig. 9 *A*. The measured rate of uptake from the apical and the basolateral surface were essentially comparable with those of the Eph4 cell line expressing the receptor alone (clone control) as well as the Eph4 cell line expressing WT rab17 (data not shown), suggesting that none of the rab17 proteins affected these steps. In contrast, we found that rab17Q77L and rab17N132I mutants caused a ~2.5-fold increase in basolateral to apical transcytosis of the receptor (Fig. 9 *B*). This effect was neither seen in the Eph4 clone control nor in the cells expressing WT rab17 (not shown), and was detectable only after 20 min or longer incubation time. It is important to note that, because the results are expressed as a percentage of Fab fragment initially bound and because the counts of basolateral binding and internalization are higher than the corresponding ones for the apical side, the magnitude of the basolateral to apical transcytosis is underestimated compared with that for the opposite direction (Fig. 9 *B*). This is not the case, as in Eph4 parental cells and the line expressing WT rab17, the flow of transport in both the basolateral to apical and the apical to basolateral transcytosis was quantitatively similar (see legend to Fig. 9). The rab17Q77L overexpressing cell line showed just a moder-

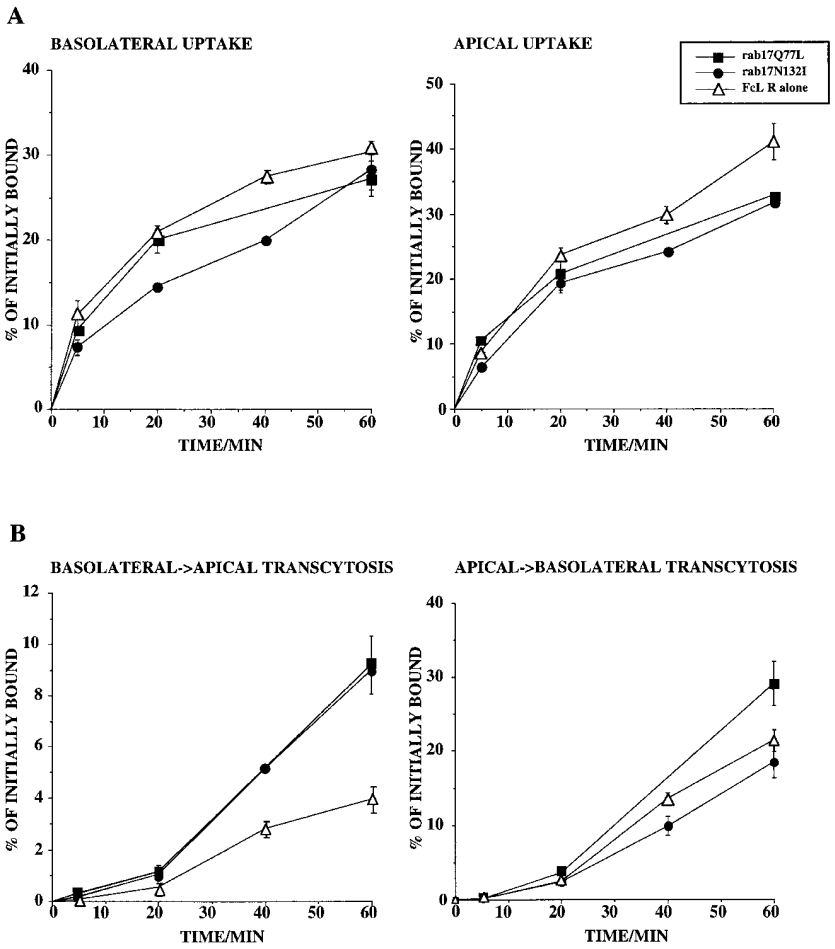

Figure. 9. Kinetic analysis of the FcLR 5-27 chimeric receptor in Eph4 cell lines overexpressing rab17 mutants. Filter-grown Eph4 cells harboring Mx-FcLR 5-27 chimeric receptor alone (△), or together with Mx-rab17Q77L (■), or Mx-rab17N132I (●) were induced with interferon. Internalized and transcytosed Fab fragment were measured as described in Materials and Methods. Each time point represents the mean of duplicate samples: the experiments were repeated three times with similar results. Note that because the results are expressed as a percentage of total receptor number, the magnitude of the basolateral to apical transcytosis appears much smaller that that for the opposite direction. In reality, the actual ECL counts are very similar in both the basolateral to apical and the apical to baolateral transcytosis (e.g., 6,525,353 ECL counts for B→A versus 5,559,544 for A→B in parental Eph4 cells).

ate increase in apical to basolateral transcytosis, and this was not seen in the case of the Eph4 clone control. The above experiments were carried out on several independently derived inducible lines with similar results. These data indicate that, as for TR, the rab17 mutants increase the basolateral to apical transcytosis of the FcLR 5-27.

Rab17 Mutants Affect Apical Recycling of the FcLR 5-27

Transport to the recycling endosome requires the presence of microtubules (Hunziker et al., 1990; Apodaca et al., 1994). To determine whether the rab17 mutants affect this step, we examined the effect of nocodazole. We observed that treatment of Eph4 with nocodazole for 3 h at 37°C caused only a partial disruption of microtubules. Nevertheless, nocodazole decreased basolateral to apical transcytosis of the FcLR 5-27 in the Eph4 control clone by 40%. However, neither preincubation with nocodazole before internalization nor treatment for 1 h at 4°C after internalization of biotinylated Fab fragments for 30 min from the basolateral side prevented the stimulatory effect of the rab17 mutant proteins on transcytosis (data not shown). These results would argue that the Rab17 mutant proteins may affect transport beyond the nocodazole-sensitive step, from the apical recycling endosome to the apical plasma membrane, i.e., recycling.

To test this hypothesis, biotinylated Fab fragments were first internalized from the apical surface of Eph4 cells for 10 min at 37°C. Cells were then incubated for an additional 10 min at 37°C in the presence of nonbiotinylated ligand to chase out the receptor from the apical sorting endosome and preferentially label the apical recycling endosome (Apodaca et al., 1994). The remaining surface-bound label was stripped by incubation with the impermeant reducing agent MesNa. The fraction of Fab fragment recycled back to the apical surface or transported to the basolateral side was eluted by low pH wash at 4°C. As shown in Fig. 10, expression of both rab17Q77L and rab17N132I mutants caused a marked increase of apical recycling when compared with the Eph4 cell line expressing the receptor alone. This effect was paralleled by a faster depletion of internal receptor in both mutant lines. In contrast, transport to the basolateral surface proceeded with similar kinetics and to a similar extent in all cell lines. These data suggest that the Rab17 mutant proteins stimulate recycling of the receptor from the apical recycling endosome to the apical surface.

Discussion

In this study we have addressed the intracellular localization and function of rab17, the first small GTPase that has been shown to be induced upon cell polarization (Lütcke et al., 1993). First, we report that rab17 associates with the perinuclear recycling endosome when ectopically expressed

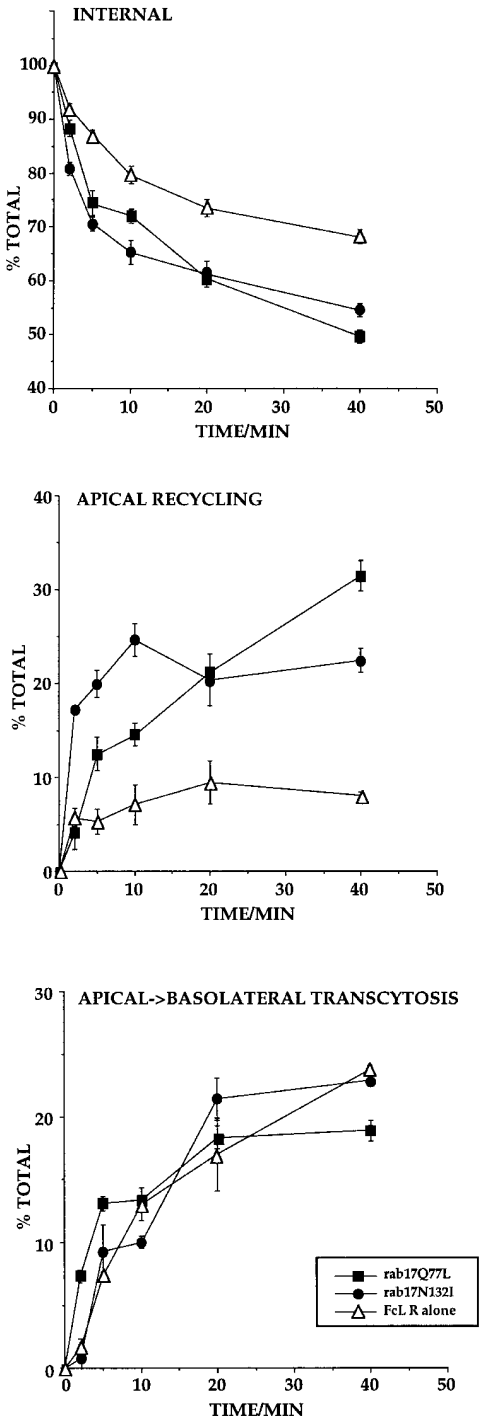

Figure 10. Kinetic analysis of apical recycling and basolateral transcytosis of the FcLR 5-27 chimeric receptor in Eph4 cell lines overexpressing rab17 mutants. Filter-grown Eph4 cells harboring Mx-FcLR 5-27 chimeric receptor alone (△), or together with Mx-rab17Q77L (■), or Mx-rab17N132I (●), were induced with interferon. Cells were allowed to internalize biotinylated Fab fragments from the apical side for 10 min at 37°C and further incubated for 10 min at 37°C in the presence of 100-fold molar excess of nonbiotinylated Fab fragments to chase the ligand to the apical recycling endosome (Apodaca et al., 1994). Apically recycled, basolaterally transcytosed, and internalized ligands were measured as described in Materials and Methods. Each time point represents the mean of duplicate samples.

in nonpolarized BHK-21 cells. Second, rab17 is localized to the apical recycling compartment in polarized Eph4 cells. Third, consistent with this localization, we show that the expression of rab17 mutants enhance basolateral to apical transcytosis. Fourth, apical recycling is stimulated by rab17 mutants. Our results provide support to the hypothesis that the recycling endosome of nonpolarized cells corresponds to the apical recycling endosome of polarized cells and further indicate that rab17 regulates transport through this compartment.

Detailed morphological and biochemical studies have suggested that the early endosome and the recycling endosome are functionally and morphologically distinct compartments (Gruenberg and Maxfield, 1995). The recycling endosome consists of tightly clustered narrow tubules organized about the centrosome and localized close to the nucleus. It is characterized by the presence of recycling molecules (e.g., TR) and by the exclusion of proteins destined for degradation (Dunn et al., 1989; Ghosh and Maxfield, 1995). Although several morphological and functional similarities suggest an analogy with the apical recycling endosome described in polarized cells (Barroso and Sztul, 1994; Apodaca et al., 1994), the lack of specific markers for the latter compartment has hampered comparisons at the molecular level. One of the main findings of our study is that rab17 is highly concentrated on the apical recycling endosome, further strengthening the homology with the recycling endosome in nonpolarized cells. First, previous immunofluorescence and immunoelectron microscopic studies on mouse kidney sections revealed the presence of rab17 on tubular elements located just below the apical brush border. These structures, also referred to as apical dense tubules, have been previously implicated in transcytosis and apical recycling (Christensen, 1982; Nielsen et al., 1985). Second, immunoelectron microscopy analysis of nonpolarized cells showed that rab17 is present on vesicular and tubular structures, which surround the centrosome and underly the plasma membrane, as well as multivesicular endosomes (Fig. 4). Rab17 expressed in fully polarized Eph4 cells specifically associates with vesicular and tubular structures concentrated at the apical pole of the cell (Fig. 3). Third, a fraction of TR internalized from the basolateral side accesses the rab17-positive apical endosome (Figs. 5 and 6), in agreement with previous studies in MDCK cells (Apodaca et al., 1994), although Barroso failed to detect Tf in this compartment (Barroso and Sztul, 1994). The apical recycling endosome may be distinct from the apical and the basolateral early endosomes but connected with them via vesicular traffic. Alternatively, the existence of a single continuous endomembrane system where apical and basolateral membrane proteins are endocytosed from both plasma membrane domains and then recycled to the surface or transcytosed has been proposed (Odorizzi et al., 1996). The latter view was based on the observation that TR extensively codistributes in endosomal elements when internalized from either surface. This view is inconsistent with the observation that TR shows extensive but not complete colocalization with rab17 by confocal immunofluorescence microscopy. We cannot, however, discriminate at this level of resolution between the presence of distinct endosomal compartments and subdomains within the same compartment.

Based on the localization studies, rab17 would be expected to specifically regulate traffic primarily through the apical recycling endosome. Our studies following the traffic of two membrane-bound markers, the basolateral recycling TR and the transcytosing FcLR 5-27 (Matter et al., 1993) in polarized Eph4 cells support this model. We found that neither the basolateral uptake nor the basolateral recycling were affected by the overexpression of WT or mutant rab17 proteins. Moreover, the lack of effect on FcLR 5-27 uptake seems to exclude a role for rab17 in apical endocytosis. In contrast, whereas the WT protein had no effect, both rab17 mutants specifically affected the basolateral to apical transcytotic route, as shown by the increased apical transport of the FcLR 5-27 and by the increased amount of apically released Tf. To investigate the putative site of rab17 function we intended to take advantage of the 17°C temperature block (Hunziker et al., 1990; Barroso and Sztul, 1994) to accumulate the transcytosing FcLR 5–27 in the apical recycling endosome and analyze the kinetics of transport towards the apical plasma membrane in the presence of the rab17 mutant proteins. Unfortunately, this approach failed because Eph4 cells showed a dramatic block in transport activity that could not be rescued by shifting the temperature to 37°C. Therefore, we turned to nocodazole, which has been used as an inhibitor of basolateral to apical transcytosis of the pIgR and Fc receptors (Hunziker et al., 1990; Apodaca et al., 1994). Although nocodazole only partially disrupted the microtubule network in Eph4 cells, it inhibited basolateral to apical transcytosis. However, the stimulatory effect by the rab17 mutant proteins was not prevented by treatment with nocodazole, suggesting a role for rab17 at, or beyond, the apical recycling endosome to the apical cell surface. Consistent with the latter possibility, both rab17 mutants increase apical recycling of the FcLR 5-27 suggesting that the increased transcytosis may be due to an increase in transport from the apical recycling endosome towards the apical plasma membrane. In accordance with this, both mutant proteins altered the apical to basolateral distribution of the FcLR 5-27, increasing the fraction of receptor present on the apical plasma membrane. Our results, therefore, suggest that rab17 may be induced during cell polarization (Lütcke et al., 1993) to modify the trafficking properties of the recycling endosome to sustain polarized sorting.

By confocal microscopy the bulk of rab17 is on the recycling endosome but a fraction of the protein is also localized on peripheral vesicular structures. The nature of these vesicles is not clear but they may correspond to transport intermediates directed to, or originating from, the recycling endosome. Besides apical recycling and transcytosis, we cannot exclude on the basis of the localization pattern other additional functions in transport steps connecting the apical recycling endosome with the sorting endosomes. The task of pinpointing these transport steps may thus prove hard by in vivo studies due to the difficulty in synchronizing traffic through the different compartments. Addressing this question would in all likelihood require the use of an in vitro transport assay. Permeabilized MDCK cells have proven to be a powerful tool to study the molecular requirements in the biosynthetic and endocytic transport routes (Podbilewicz and Mellman, 1990; Pimplikar and Simons, 1993; Pimplikar et al., 1994) and, more specifically, in the transcytotic pathway (Apodaca et al., 1996).

It is interesting to note that the amplitude of the effect seen for the two marker proteins is different, being higher in the case of the FcLR 5-27 compared with that for TR. It thus appears that membrane-bound markers which are trafficking along functionally different pathways (transcytosis versus basolateral recycling) are not affected to the same extent. TR exhibits high polarity (Fuller and Simons, 1986) and, compared with the FcLR 5-27, the accuracy and efficiency of its basolateral targeting is presumably ensured by its sorting signals in conjunction with the sorting properties of the basolateral early endosomes. Only a minor fraction of TR would be apically missorted out of the small fraction that has eluded the first round of sorting in the basolateral early endosomes and has gained the recycling endosome. This view is supported by a recent study showing that the majority (~70%) of basolaterally internalized TR is efficiently recycled to the basolateral plasma membrane from the basolateral sorting endosome before reaching the apical recycling endosome (Sheff, D., E. Daro, I. Mellman, manuscript submitted for publication). Two observations are consistent with this model. First, no effect on the Tf cycle was observed in nonpolarized cells expressing WT rab17 and rab17 mutants. Alterations in the kinetics of transport from the recycling endosome would, in fact, be too small to be detected, because the cell is not differentiated into functionally and spatially distinct apical and basolateral domains as in polarized cells. Second, Tf slowly accumulated in the rab17-positive recycling endosome when this compartment relocated above the nucleus in polarized cells (Fig. 5).

The fact that two distinct mutations, one causing a defect in GTP hydrolysis and the other decreasing nucleotide binding (Wittinghofer and Valencia, 1995), yield similar perturbations on the pathway when introduced in rab17 is not unprecedented in the case of rab proteins. For example, analogous mutants of rab3a exert the same inhibitory function on Ca^{2+}-dependent exocytosis (Johannes et al., 1994). In the case of rab6 both the T27N and Q72L mutants induce the intracellular accumulation of secretory proteins (Martinez et al., 1994). Although the mutant proteins may affect different steps of the GTP cycle, both cause the same transport deficiency. It is unlikely that the rab17 mutants used in our studies may act unspecifically by perturbing the general transport machinery, i.e., titrating out a common regulatory factor for rab proteins such as GDP dissociation inhibitor (GDI). Similar mutants have proven to be very specific in many other studies (for reviews see Pfeffer, 1994; Nuoffer and Balch, 1994; Novick and Zerial, 1997). Furthermore, whereas both apical and basolateral uptake are stimulated by the overexpression of rab5 (Bucci et al., 1994), the expression of rab17 has neither consequences for these steps (Fig. 9, *A* and *B*) nor for Tf recycling in nonpolarized cells (Fig. 7, *A* and *B*).

Several rab proteins have now been localized to compartments of the endocytic pathway and functional studies have shown that they regulate distinct and often sequential transport steps. Rab5, for instance, controls the incoming endocytic traffic from the plasma membrane to the sorting endosome (Bucci et al., 1992) whereas rab4 seems to operate on the fast cycle of recycling (Diaz et al., 1988;

van der Sluijs et al., 1992*a*; Daro et al., 1996). Moreover, rab11 has been recently localized to the recycling endosome and appears to be required for recycling through this compartment in nonpolarized cells (Ullrich et al., 1996). Its role in polarized cells has not yet been determined, but one possibility is that it may affect the basolateral recycling pathway. In this context rab17 would be required, and consequently induced, to confer the polarized sorting function to the recycling endosome. In conclusion, the identification of rab17 as regulator of transport through the apical recycling compartment provides a functional marker for this compartment, which should facilitate the study of protein sorting in polarized cells.

We thank Ernst Reichmann and Hartmut Beug (Research Institute of Molecular Pathology, Vienna, Austria) for providing the mouse epithelial Eph4 cell line. We are grateful to Bei Yu for technical assistance and Cayetano Gonzalez, Sigrid Reinsch, and Ernst Stelzer for advice on confocal microscopy. We acknowledge Anne Lütcke for help in the initial stages of setting up the transport assay in polarized cells. We thank W. Hunziker (Lausanne, Switzerland) for discussions and sharing unpublished data. We thank Bernard Hoflack, Sigrid Reinsch, and Kai Simons for critical reading of the manuscript.

This work was supported by grants from the Human Frontier Science Program to M. Zerial (RG-432/96) and R.G. Parton (RG-355/94), European Community grants: Human Capital and Mobility, and Training and Mobility of Reseacheis to M. Zerial, HCM, and TMR grants to M. Zerial (ERB-CT94-0592 and ERB-CT96-0020), and a National Institutes of Health grant to I. Mellman (GM29765).

Received for publication 29 September 1997 and in revised form 7 January 1998.

References

Apodaca, A., L.A. Katz, and K.E. Mostov. 1994. Receptor-mediated transcytosis of IgA in MDCK cells is via apical recycling endosomes. *J. Cell Biol.* 125: 67–86.

Apodaca, G., M.H. Cardone, S.W. Whiteheart, B.R. DasGupta, and K.E. Mostov. 1996. Reconstitution of transcytosis in SLO-permeabilized MDCK cells: existence of an NSF-dependent fusion mechanism with the apical surface of MDCK cells. *EMBO (Eur. Mol. Biol. Organ.) J.* 15:1471–1481.

Arnheiter, H., S. Skuntz, M. Noteborn, S. Chang, and E. Meier. 1990. Transgenic mice with intracellular immunity to infuenza virus. *Cell.* 62:51–61.

Bachiller, D., and U. Rüther. 1990. Inducible expression of the proto-oncogene c-fos in transgenic mice. *Arch. Geschwulstforsch.* 60:357–360.

Barroso, M., and E.S. Sztul. 1994. Basolateral to apical transcytosis in polarized cells is indirect and involves BFA and trimeric G protein sensitive passage through the apical endosome. *J. Cell Biol.* 124:83–100.

Bomsel, M., K. Prydz, R.G. Parton, J. Gruenberg, and K. Simons. 1989. Endocytosis in filter-grown Madin-Darby canine kidney cells. *J. Cell Biol.* 109: 3243–3258.

Bucci, C., R.G. Parton, I.H. Mather, H. Stunnenberg, K. Simons, B. Hoflack, and M. Zerial. 1992. The small GTPase rab5 functions as a regulatory factor in the early endocytic pathway. *Cell.* 70:715–728.

Bucci, C., A. Wandinger-Ness, A. Lütcke, M. Chiariello, C.B. Bruni, and M. Zerial. 1994. Rab5a is a common component of the basolateral and apical endocytic machinery in polarized epithelial cells. *Proc. Natl. Acad. Sci. USA.* 91:5061–5065.

Chavrier, P., R.G. Parton, H.P. Hauri, K. Simons, and M. Zerial. 1990. Localization of low molecular weight GTP binding proteins to exocytic and endocytic compartments. *Cell.* 62:317–329.

Christensen, E.I. 1982. Rapid membrane recycling in proximal tubule cells. *Eur. J. Cell Biol.* 29:43–49.

Daro, E.P., P. van der Sluijs, T. Galli, and I. Mellman. 1996. Rab4 and cellubrevin define different early endosome populations on the pathway of transferrin receptor recycling. *Proc. Natl. Acad. Sci. USA.* 93:9559–9564.

Diaz, R., L. Mayorga, and P. Stahl. 1988. *In vitro* fusion of endosomes after receptor-mediated endocytosis. *J. Biol. Chem.* 263:6093–6100.

Dunn, K.W., T.E. McGraw, and F.R. Maxfield. 1989. Iterative fractionation of recycling receptors from lysosomally destined ligands in an early sorting endosome. *J. Cell Biol.* 109:3303–3314.

Fujita, M., F. Reinhart, and M. Neutra. 1990. Convergence of apical and basolateral endocytic pathways at apical late endosomes in absorptive cells of suckling rat ileum *in vivo*. *J. Cell Sci.* 97:385–394.

Fuller, S.E., and K. Simons. 1986. Transferrin receptor polarity and recycling accuracy in tight and leaky strains of Madin-Darby canine kidney cells. *J. Cell Biol.* 103:1767–1779.

Galli, T., T. Chilcote, O. Mundigl, T. Binz, H. Niemann, and P. De Camilli. 1994. Tetanus toxin-mediated cleavage of cellubrevin impairs exocytosis of transferrin receptor-containing vesicles in CHO cells. *J. Cell Biol.* 125:1015–1024.

Geller, A.I., and X.O. Breakefield. 1988. A defective HSV-1 vector expresses Escherichia coli b-galactosidase in cultured peripheral neurons. *Science.* 241: 1667–1669.

Ghosh, R.N., and F.R. Maxfield. 1995. Evidence for nonvectorial, retrograde transferrin trafficking in the early endosomes of HEp2 cells. *J. Cell Biol.* 128: 549–561.

Ghosh, R.N., D.L. Gelman, and F.R. Maxfield. 1994. Quantification of low density lipoprotein and transferrin endocytic sorting in HEp2 cells using confocal microscopy. *J. Cell Sci.* 107:2177–2189.

Gruenberg, J., and F.R. Maxfield. 1995. Membrane transport in the endocytic pathway. *Curr. Opin. Cell Biol.* 7:552–563.

Hopkins, C.R. 1983*a.* Intracellular routing of transferrin and transferrin receptor in epidermoid carcinoma A431. *Cell.* 35:321–330.

Hopkins, C.R., A. Gibson, M. Shipman, and K. Miller. 1990. Movement of internalized ligand-receptor complexes along a continuous endosomal reticulum. *Nature.* 346:335–339.

Hopkins, C.R., A. Gibson, M. Shipman, D.K. Strickland, and I.S. Trowbridge. 1994. In migrating fibroblasts, recycling receptors are concentrated in narrow tubules in the pericentriolar area, and then routed to the plasma membrane of the leading lamella. *J. Cell Biol.* 125:1265–1274.

Hug, H., M. Costas, P. Staeheli, M. Aebi, and C. Weissmann. 1988. Organization of the murine MX gene and characterization of its Interferon- and virus-inducible promoter. *Mol. Cell. Biol.* 8:3065–3079.

Hughson, E.J., and C.R. Hopkins. 1990. Endocytic pathways in polarized Caco-2 cells: identification of an endosomal compartment accessible from both apical and basolateral surfaces. *J. Cell Biol.* 110:337–348.

Hunziker, W., P. Male, and I. Mellman. 1990. Differential microtubule requirements for transcytosis in MDCK cells. *EMBO (Eur. Mol. Biol. Organ.) J.* 9:3515–3525.

Hunziker, W., and I. Mellman. 1989. Expression of macrophage-lymphocyte Fc receptors in MDCK cells: polarity and transcytosis differ for isoforms with or without coated pit localization domains. *J. Cell Biol.* 109:3291–3302.

Johannes, L., P.-M. Lledo, M. Roa, J.-D. Vincent, J.-P. Henry, and F. Darchen. 1994. The GTPase Rab3a negatively controls calcium-dependent exocytosis in neuroendocrine cells. *EMBO (Eur. Mol. Biol. Organ.) J.* 13:2029–2037.

Knight, A., E. Hughson, C.R. Hopkins, and D.F. Cutler. 1995. Membrane protein trafficking through the common apical endosome compartment of polarized Caco-2 cells. *Mol. Biol. Cell.* 6:597–610.

Kozak, M. 1987. At least six nucleotides preceding the AUG initiator codon enhance translation in mammalian cells. *J. Mol. Biol.* 196:947–950.

Landt, O., H.-P. Grunert, and U. Hahn. 1990. A general method for rapid site-directed mutagenesis using the polymerase chain reaction. *Gene.* 96:125–128.

Lim, F., D. Hartley, P. Starr, S. Song, L. Yu, Y. Wang, and A.I. Geller. 1996. Generation of high-titer defective HSV-1 vectors using an IE 2 deletion mutant and quantitative study of expression in cultured cortical cells. *Biotechniques.* 20:460–469.

Lütcke, A., S. Jansson, R.G. Parton, P. Chavrier, A. Valencia, L. Huber, E. Lehtonen, and M. Zerial. 1993. Rab17, a novel small GTPase, is specific for epithelial cells and is induced during cell polarization. *J. Cell Biol.* 121:553–564.

Martinez, O., A. Schmidt, J. Salaméro, B. Hoflack, M. Roa, and B. Goud. 1994. The small GTP-binding protein rab6 functions in intra-Golgi transport. *J. Cell Biol.* 127:1575–1588.

Matter, K., W. Hunziker, and I. Mellman. 1992. Basolateral sorting of the LDL receptor in MDCK cells: the cytoplasmic domain contains two tyrosine-dependent targeting determinants. *Cell.* 71:741–753.

Matter, K., A. Whitney, E.M. Yamamoto, and I. Mellman. 1993. Comman signals control low density lipoprotein receptor sorting in endosomes and the Golgi complex of MDCK cells. *Cell.* 74:1053–1064.

McMahon, H.T., Y.A. Ushkaryov, L. Edelmann, E. Link, T. Binz, H. Niemann, R. Jahn, and T.C. Sudhof. 1993. Cellubrevin is a ubiquitous tetanus-toxin substrate homologous to a putative synaptic vesicle fusion protein. *Nature.* 364:346–349.

Mellman, I. 1996. Endocytosis and molecular sorting. *Annu. Rev. Cell Dev. Biol.* 12:575–625.

Mellman, I., and H. Plutner. 1984*a.* Internalization and degradation of macrophage Fc receptors bound to polyvalent immune complexes. *J. Cell Biol.* 98:1170–1176.

Mellman, I., H. Plutner, and P. Ukkonen. 1984*b.* Internalization and rapid recycling on macrophage Fc receptors tagged with monovalent antireceptor antibody: possible role of a prelysosomal compartment. *J. Cell Biol.* 98:1163–1169.

Mostov, K., G. Apodaca, B. Aroeti, and C. Okamoto. 1992. Plasma membrane protein sorting in polarized epithelial cells. *J. Cell Biol.* 116:577–583.

Mostov, K.E. 1994. Transepithelial transport of immunoglobulins. *Annu. Rev. Immunol.* 12:63–84.

Mostov, K.E., and M.H. Cardone. 1995. Regulation of protein traffic in polarized epithelial cells. *BioEssay.* 17:129–138.

Murphy, C., P. Zacchi, G.P. Parton, M. Zerial, and F. Lim. 1997. HSV infection of polarized epithelial cells on filters supports: implications for transport assays and protein localization. *Eur. J. Cell Biol.* 72:278–281.

Musch, A., H. Xu, D. Shields, and E. Rodriguez-Boulan. 1996. Transport of vesicular stomatitis virus G protein to the cell surface is signal mediated in polarized and nonpolarized cells. *J. Cell Biol.* 133:543–558.
Nelson, W.J. 1992. Regulation of cell surface polarity from bacteria to mammals. *Science.* 258:948–955.
Nielsen, J.T., S. Nielsen, and E.I. Christensen. 1985. Transtubular transport of proteins in rabbit proximal tubules. *J. Ultrastruct. Res.* 92:133–145.
Novick, P., and M. Zerial. 1997. The diversity of rab proteins in vesicle transport. *Curr. Opin. Cell Biol.* 9:496–504.
Nuoffer, C., and W.E. Balch. 1994. GTPases: multifunctional molecular switches regulating vesicular traffic. *Ann. Rev. Biochem.* 63:949–990.
Odorizzi, G., A. Pearse, D. Domingo, I.S. Trowbridge, and C.R. Hopkins. 1996. Apical and basolateral endosomes of MDCK cells are interconnected and contain a polarized sorting mechanism. *J. Cell Biol.* 135:1–14.
Parton, R.G., K. Prydz, M. Bomsel, K. Simons, and G. Griffiths. 1989. Meeting of the apical and basolateral endocytic pathways of the Madin-Darby canine kidney cell in late endosomes. *J. Cell Biol.* 109:3259–3272.
Pfeffer, S.R. 1994. Rab GTPases: master regulators of membrane trafficking. *Curr. Opin. Cell Biol.* 6:522–526.
Pimplikar, S.W., E. Ikonen, and K. Simons. 1994. Basolateral protein transport in Streptolysin O-permeabilized MDCK cells. *J. Cell Biol.* 125:1025–1035.
Pimplikar, S.W., and K. Simons. 1993. Regulation of apical transport in epithelial cells by a Gs class of heterotrimeric G protein. *Nature.* 362:456–458.
Podbilewicz, B., and I. Mellman. 1990. ATP and cytosol requirements for transferrin recycling in intact and disrupted MDCK cells. *EMBO (Eur. Mol. Biol. Organ.) J.* 9:3477–3487.
Reichmann, E., R. Ball, B. Groner, and R.R. Friis. 1989. New mammary epithelial and fibroblastic cell clones in coculture form structures competent to differentiate fuctionally. *J. Cell Biol.* 108:1127–1138.
Reichmann, E., H. Schwarz, E.M. Deiner, I. Leitner, M. Eilers, J. Berger, M. Busslinger, and H. Beug. 1992. Activation of an inducible c-FosER fusion protein causes loss of epithelial polarity and triggers epithelial-fibroblastoid cell conversion. *Cell.* 71:1103–1116.
Rodman, J.S., R.W. Mercer, and P.D. Stahl. 1990. Endocytosis and transcytosis. *Curr. Opin. Cell Biol.* 2:664–672.
Rodriguez-Boulan, E., and S.K. Powell. 1992. Polarity of epithelial and neuronal cells. *Annu. Rev. Cell Biol.* 8:395–427.
Simons, K., and A. Wandinger-Ness. 1990. Polarized sorting in epithelia. *Cell.* 62:207–210.
Smythe, E., T.E. Redelmeier, and S.L. Schmid. 1992. Receptor-mediated endocytosis in perforated cells. *Methods. Enzymol.* 219:223–234.
Stenmark, H., C. Bucci, and M. Zerial. 1995. Expression of Rab GTPases using recombinant vaccinia virus. *Methods Enzymol.* 257:155–164.
Strange, R., F. Li, R.R. Friis, E. Reichmann, B. Haenni, and P.H. Burri. 1991. Mammary epithelial differentiation in vitro: minimum requirements for a functional response to hormonal stimulation. *Cell growth Differ.* 2:549–559.
Ullrich, O., S. Reinsch, S. Urbe, M. Zerial, and R.G. Parton. 1996. Rab11 regulates recycling through the pericentriolar recycling endosome. *J. Cell Biol.* 135:913–924.
Ullrich, O., H. Stenmark, K. Alexandrov, L.A. Huber, K. Kaibuchi, T. Sasaki, Y. Takai, and M. Zerial. 1993. Rab GDP dissociation inhibitor as a general regulator for the membrane association of rab proteins. *J. Biol. Chem.* 268: 18143–18150.
Unkeless, J.C. 1979. Characterization of a monoclonal antibody directed against mouse macrophage and lymphocytes Fc receptors. *J. Exp. Med.* 150: 580–596.
van der Sluijs, P., M. Hull, P. Webster, P. Mâle, B. Goud, and I. Mellman. 1992*a.* The small GTP-binding protein rab4 controls an early sorting event on the endocytic pathway. *Cell.* 70:729–740.
Watts, C., and M. Marsh. 1992. Endocytosis: what goes in and how? *J. Cell Sci.* 103:1–8.
Wittinghofer, A., and A. Valencia. 1995. In Guidebook to the Small GTPase. M. Zerial and L.A. Huber, editors. Oxford University Press, Oxford, U.K. 20–29.
Woodroofe, C., W. Muller, and U. Rüther. 1992. Long-term consequences of interleukin-6 overexpression in transgenic mice. *DNA Cell Biol.* 11:587–592.
Yamashiro, D.J., S.R. Fluss, and F.R. Maxfield. 1983. Acidification of endocytic vesicles by an ATP-dependent proton pump. *J. Cell Biol.* 97:929–934.
Yamashiro, D.J., and F.R. Maxfield. 1984. Segregation of transferrin to a mildly acidic (pH 6.5) para-Golgi compartment in the recycling pathway. *Cell.* 37: 389–400.
Yamashiro, D.J., and F.R. Maxfield. 1987. Acidification of morphologically distinct endosomes in mutant and wild-type Chinese hamster ovary cells. *J. Cell Biol.* 105:2723–2733.
Yoshimori, T., P. Keller, M.G. Roth, and K. Simons. 1996. Different biosynthetic routes to the plasma membrane in BHK and CHO cells. *J. Cell Biol.* 133:247–256.
Zerial, M., P. Melancon, C. Schneider, and H. Garoff. 1986. The transmembrane segment of the human transferrin receptor functions as a signal peptide. *EMBO (Eur. Mol. Biol. Organ.) J.* 5:1543–1550.